Neural Comput & Applic (2014) 25:557–572
DOI 10.1007/s00521-013-1520-x

ORIGINAL ARTICLE

Lithium-ion battery remaining useful life estimation based on fusion nonlinear degradation AR model and RPF algorithm

Datong Liu · Yue Luo · Jie Liu · Yu Peng · Limeng Guo · Michael Pecht

Received: 12 April 2013 / Accepted: 20 November 2013 / Published online: 3 December 2013

Abstract The lithium-ion battery cycle life prediction with particle filter (PF) depends on the physical or empirical model. However, in observation equation based on model, the adaptability and accuracy for individual battery under different operating conditions are not fully considered. Therefore, a novel fusion prognostic framework is proposed, in which the data-driven time series prediction model is adopted as observation equation, and combined to PF algorithm for lithium-ion battery cycle life prediction. Firstly, the nonlinear degradation feature of the lithium-ion battery capacity degradation is analyzed, and then, the nonlinear accelerated degradation factor is extracted to improve prediction ability of linear AR model. So an optimized nonlinear degradation autoregressive (ND–AR) time series model for remaining useful life (RUL) estimation of lithium-ion batteries is introduced. Then, the ND–AR model is used to realize multi-step prediction of the battery capacity degradation states. Finally, to improve the uncertainty representation ability of the standard PF algorithm, the regularized particle filter is applied to design a fusion RUL estimation framework of lithium-ion battery. Experimental results with the lithium-ion battery test data from NASA and CALCE (The Center for Advanced Life Cycle Engineering, the University of Maryland) show that the proposed fusion prognostic approach can effectively predict the battery RUL with more accurate forecasting result and uncertainty representation of probability density distribution (pdf).

Keywords Lithium-ion battery · Fusion prognostics · Data-driven prognostics · ND–AR · RPF

D. Liu (✉) · Y. Peng · L. Guo
Department of Automatic Test and Control, Harbin Institute of Technology, Harbin 150080, China
e-mail: liudatong@hit.edu.cn

Y. Luo
Beijing System Design Institute of Electro-Mechanic Engineering, Beijing 100854, China

J. Liu
Department of Mechanical and Aerospace Engineering, Carleton University, Ottawa, ON K1S 5B6, Canada

M. Pecht
CALCE, The University of Maryland, College Park, MD 20742, USA

1 Introduction

Due to high energy density, high galvanic potential, wide temperature range, low self-discharge rate and long lifetime, lithium-ion batteries are core components in a wide variety of systems. Therefore, the reliability of lithium-ion batteries becomes a subject of great interest to the electronics industry [1, 2]. With the challenges of safety management, charging and discharging control, performance degradation of the lithium-ion battery, capacity fade and remaining useful life (RUL) estimation has become a hotspot and challenging issue in the fields of reliability engineering, automatic test, power sources, electric vehicles, etc. As a result, lithium-ion battery RUL prognostics became the hot issues in the prognostics and health management (PHM) of electronics [3, 4]. The prognostics and RUL estimation entails the use of the current and previous system states to forecast the future states of the battery system. Reliable predicted information can be used to schedule repairs and maintenance in advance and provide an alarm before faults reach critical levels so as to prevent performance degradation, malfunction or even catastrophic failures [5, 6].

Generally, among the various approaches of battery RUL prognostics, it can be generally classified into two categories: model-based approaches and data-driven approaches [1, 7]. Model-based approaches typically involve building physical models (or mathematical and chemistry models) to describe the physics of the system states and failure evolvement. The physical understanding of the system is usually incorporated into the estimation of system states and RUL [8]. However, model-based may not be suitable for many actual applications in which the physical parameters and failure modes may vary under various operation conditions [9]. It is usually difficult to obtain suitable physical model to describe the system dynamic characteristics; otherwise, it is hard to identify the adaptive parameters for complicated model of complex systems. Moreover, the model-based approaches cannot be applied for those complex systems in which the internal state variables are inaccessible to direct testing and monitoring with general sensors. In this case, inference has to be made from indirect measurements using techniques such as particle filter (PF) algorithm. Saha et al. [4, 10] in the Prognostics Center of Excellence (PCoE) of the NASA AMES Center has achieved the battery RUL prediction and the uncertainty representation and management with PF algorithm. To overcome the high dependence on the electrochemical impedance spectroscopy (EIS) test equipment, Saha and Goebel established an empirical degradation model which the PF is employed to update considering the coulombic efficiency factor and capacity regeneration phenomenon. Orchard et al. [11] proposed a prediction framework which combined PF and anomaly detection model for the battery capacity estimation and cycle life prediction, taking into account the power regeneration phenomenon in usage. The anomaly detection module is responsible for the detection of capacity regenerative phenomenon, and the PF method is used to realize RUL prediction. Moreover, a PF-based simplified prognostic algorithm is proposed to realize fast risk analysis and state-of-charge estimation, as a result, a real-time application is implemented [12]. However, a limitation associated with the PF-based prognostic method is that the prediction model parameters cannot be updated during the prediction period since no new monitoring data are available, as a result, the prediction accuracy cannot be satisfied in many industrial applications.

Data-driven approaches for battery prognostics extract features from the monitoring data such as current, voltage, time and impedance, using statistical and machine learning techniques to track the degradation and estimate the RUL. These data-driven methods can capture the inherent relationships and learn trends present in the data to provide RUL estimations [13]. The classical data-driven methods for system state prediction include statistical stochastic models such as the autoregressive (AR) model and autoregressive moving average (ARMA) model. With the development of computing intelligence and machine learning, more research work of data-driven prognostics have been focused on the use of flexible models for battery RUL predictions such as various types of neural networks (NNs) [14, 15], neural fuzzy (NF) systems [16], support vector machine (SVM) [10]. Data-driven methods rely on past patterns of the degradation of similar systems to forecast the future system states. The predicted accuracy depends on both the quantity of modeling data samples and the history knowledge involved in the monitoring data [5]. Another principal disadvantage of data-driven methods is that the prognostic process is usually opaque, and the model is invisible to users.

To overcome the limitation of the data-driven approaches and model-based approaches, the fusion prognostics became the research focus to improve the RUL prediction performance. Kozlowski [17] proposed a data-driven battery RUL prediction approach that combined three predictors—autoregressive and moving average (ARMA) model, neural networks and fuzzy—to achieve a fusion prognostic method. Liu et al. [18] proposed a fusion prognostic framework to increase the system long-term prediction performance. Saha et al. [19] presented a combined battery RUL estimation method with the relevance vector machine (RVM) and PF algorithm. The PF is used to realize the parameters identification of the RVM model. An ensemble model for predicting the RUL of lithium-ion battery is introduced by combining the fused empirical exponential and polynomial regression model and PF algorithm [20]. The PF is applied to adjust the parameters of the fused regression model online to track the degradation trend of the battery cycle life.

To address the uncertainty representation ability of PF algorithm and integrate the advantages of data-driven approach and model-based approach, respectively, this research work proposed a novel fusion prognostic framework for lithium-ion battery RUL prediction. The developed framework aims to integrate the strengths of the data-driven prognostic method and the model-based PF approach for a more flexible and high-performance prediction. The proposed fusion framework is new in the following aspects: (1) An optimized nonlinear degradation autoregressive (ND–AR) model is proposed for the multi-step state prediction of lithium-ion battery, which achieves low computing complexity and reflect the "accelerated" degradation trend in the latter battery cycle lifetime. (2) Data-driven ND–AR model is adopted as the observation equation of the regularized particle filter (RPF) to improve the prediction and uncertainty representation performance, which is a novel fusion implementation compared with the fusion approaches mentioned above. (3) A fusion

prognostic framework combined ND–AR model and RPF algorithm is presented for battery RUL estimation to improve the prognostic effectiveness and efficiency.

This paper is organized as follows. In Sect. 2, the related prediction model including AR model and PF/RPF algorithm is introduced. The proposed ND–AR model and the fusion prognostic framework are described in detail in Sect. 3. The effectiveness of the proposed fusion prognostics framework is demonstrated via battery RUL prediction experiments and evaluations with two lithium-ion battery data sets in Sect. 4. A summary of important observations and conclusive remarks as well as future work are given in Sect. 5.

2 Related work

2.1 AR model

Time series analysis and prediction based on stochastic process theory and mathematical statistics has been widely applied in signal processing, intelligent information analysis and PHM and so on. In the engineering field, the AR model is used more extensive than the moving average (MA) model and the ARMA model, because the parameter identification of the AR model is relatively simple, as well as the computing complexity is low. Furthermore, it has already been proved that the MA model and ARMA model of lower order can be equivalent with AR model of much higher order [21], while the approximated prediction performance is achieved. The degradation of battery capacity data is obtained with state monitoring and testing time series data samples, which can take advantage of the AR model to realize state prediction and RUL estimation.

In the AR model, for time series $\{x_t\}$,

$$\begin{cases} x_t = \phi_1 x_{t-1} + \phi_2 x_{t-2} + \cdots + \phi_p x_{t-p} + a_t \\ \phi_p \neq 0 \end{cases} \quad (1)$$

where $\phi_i (i = 1, 2, \ldots, p)$ are autoregressive coefficients, $a_t, t = 0, \pm 1, \ldots$ is the independent white noise sequence with zero mean and constant variance σ_a^2.

The parameter p is defined as the order of the AR model, so the model can be denoted as AR(p). At this time, the AR model is described as the time series $\{x_t\}$ can equal to the linear function of the historical value and random noise. In the AR(p) model, the number of the parameters is $p + 2$, the parameters include the order p, coefficients $\phi_1, \phi_2 \ldots, \phi_p$ and σ_a^2. It is indicated from the Eq. (1) that the AR model is a type of linear prediction function.

While the AR model is applied to time series prediction, the selection of the order the model is a key issue. Because the coefficients $\{\phi_p\}$ are relevant to the order p, we should first determine the suitable order p to obtain the adaptive coefficients $\{\phi_p\}$.

In this work, the Akaike information criterion (AIC) method [22] is used for the determination of the model order. The AIC method is defined as Eq. (2).

$$AIC(p) = N \ln \sigma_p^2 + 2p \quad (2)$$

Here, p is the determination of the model order, N is the number of the data samples, σ_p^2 is the prediction variance of p order model.

The methods for parameters estimation of the AR model include the least square estimation, maximum likelihood estimation, Yule–Wallker method (autocorrelation method), the Burg method, covariance method, etc. In this paper, the Burg algorithm which can directly calculate the parameters with the observed time series is applied to achieve parameters estimation for the AR model. This algorithm can avoid the priori estimation of the autocorrelation function, as a result, the computing is simple, and the real-time performance is excellent. Especially, the Burg algorithm is suitable for the parameters estimation of short time series, which meets the requirements of the battery RUL estimation.

2.2 Particle filter algorithm for RUL prognostics

While the system states could not be directly measured, the PF algorithm provides a Bayesian learning framework to achieve states estimation and prognostics of complex systems. Given a discrete time state estimation problem, the system state vector $\mathbf{X}_k \in R^n$ evolves according to the following system model as Eq. (3)

$$\mathbf{X}_k = f_{k-1}(\mathbf{X}_{k-1}, \mathbf{w}_{k-1}) \quad (3)$$

where $f : R^n \rightarrow R^n$ is the system state transition function and $\mathbf{w}_k \in R^n$ is a noise whose known distribution is independent of time. At each discrete time instant, an observation $\mathbf{Y}_k \in R^p$ becomes available. The observation is related to the unobservable state vector via the observation equation shown as Eq. (4).

$$\mathbf{Y}_k = h_k(\mathbf{X}_k, \mathbf{v}_k) \quad (4)$$

where $h : R^n \rightarrow R^p$ is the measurement function and $\mathbf{v}_k \in R^p$ is another noise whose known distribution is independent of the system noise and time. The Bayesian learning approach to system state estimation is to recursively estimate the pdf of the unobservable state $\mathbf{X}_k$ based on a sequence of noisy measurements $\mathbf{Y}_{1:k}, k = 1, 2, \ldots, k$.

Assume that $\mathbf{X}_k$ has an initial density $p(\mathbf{X}_0)$ and the probability transition density is represented by $p(\mathbf{X}_k|\mathbf{X}_{k-1})$. The inference of the property of the states $\mathbf{X}_k$ relies on the marginal filter density $p(\mathbf{X}_k|\mathbf{Y}_{1:k})$. Suppose that the density $p(\mathbf{X}_{k-1}|\mathbf{Y}_{k-1})$ is available at step $k - 1$. The prior density

of the state at step k can then be estimated via the transition density $p(\mathbf{X}_k|\mathbf{X}_{k-1})$.

$$p(\mathbf{X}_k|\mathbf{Y}_{1:k-1}) = \int p(\mathbf{X}_k|\mathbf{X}_{k-1})p(\mathbf{X}_{k-1}|\mathbf{Y}_{1:k-1})d\mathbf{X}_{k-1} \quad (5)$$

Correspondingly, the marginal filter density is computed by the Bayesian theorem,

$$p(\mathbf{X}_k|\mathbf{Y}_{1:k}) = \frac{p(\mathbf{Y}_k|\mathbf{X}_k)p(\mathbf{X}_k|\mathbf{Y}_{1:k-1})}{p(\mathbf{Y}_k|\mathbf{Y}_{1:k-1})} \quad (6)$$

where the normalizing constant is determined by,

$$p(\mathbf{Y}_k|\mathbf{Y}_{1:k-1}) = \int p(\mathbf{Y}_k|\mathbf{X}_k)p(\mathbf{X}_k|\mathbf{Y}_{1:k-1})d\mathbf{X}_k \quad (7)$$

Equations (6–8) constitute the basis for the optimal Bayesian recursive state estimation problem. This recursive propagation of the posterior density is only a conceptual solution, which generally cannot be determined analytically [26]. If the system is linear with Gaussian noise, the above method reduces to the Kalman filter. For nonlinear/non-Gaussian systems, there are no closed-form solutions and thus numerical approximations are usually employed [23]. The PF is a technique for implementing the recursive Bayesian filtering via Monte Carlo simulations, where by the posterior density function $p(\mathbf{X}_k|\mathbf{Y}_{1:k})$ is represented by a set of random samples (particles) $\mathbf{X}_k^1, \ldots, \mathbf{X}_k^M$ and their associated weights $\pi_k^1, \ldots, \pi_k^M$, that is,

$$p(\mathbf{Y}_k|\mathbf{Y}_{1:k-1}) \approx \sum_{i=1}^{M} \pi_k^i \delta(\mathbf{X}_k - \mathbf{X}_k^i), \sum_{i=1}^{M} \pi_k^i = 1 \quad (8)$$

where M is the number of particles, the weights $\pi_k^1, \ldots, \pi_k^M$ can be recursively updated using the importance sampling with an importance density $G(\mathbf{X}_k^i|\mathbf{X}_{k-1}^i, \mathbf{Y}_k)$,

$$\pi_k^i \propto \pi_{k-1}^i \frac{p(\mathbf{Y}_k|\mathbf{X}_k^i)p(\mathbf{X}_k^i|\mathbf{X}_{k-1}^i)}{G(\mathbf{X}_k^i|\mathbf{X}_{k-1}^i, \mathbf{Y}_k)} \quad (9)$$

While the importance density is approximated as $p(\mathbf{X}_k|\mathbf{X}_{k-1})$, Eq. (9) turns to $\pi_k^i \propto \pi_{k-1}^i p(\mathbf{Y}_k|\mathbf{X}_k^1)$.

As shown in Eqs. (8) and (9), the system state in PF was represented by a series of approximate states whose pdf is closer to the actual state, and each particles has its own weight [24]. The PF algorithm is a Bayesian state estimation method based on Monte Carlo idea that can handle any nonlinear non-Gaussian problems. It estimates the system states based on state space model and the system dynamic state space model can be described as Eq. (10).

$$\begin{cases} \mathbf{X}_k = f(\mathbf{X}_{k-1}, \boldsymbol{\mu}_{k-1}) + \mathbf{w}_{k-1} \\ \mathbf{Y}_k = h(\mathbf{X}_k) + \boldsymbol{\mu}_k \end{cases} \quad (10)$$

where $\mathbf{X}_k$ is the system state variable, $\mathbf{Y}_k$ represents the observed value of $\mathbf{X}_k$, $f(\cdot)$ and $h(\cdot)$ are state transition equation and observation equation, $\boldsymbol{\mu}_{k-1}$ represents the control variables, $\mathbf{w}_k$ and $\boldsymbol{\nu}_k$ represents the system noise and observed noise, respectively.

Two steps are involved in PF: prediction (estimation) step and update (correlation) step. In prediction step, firstly, a large number of particles are generated according to a priori probability distribution. A new predicted particle can be obtained by iteration updating each particle based on state transition equation with control variables. In update step, the particles that are more closer to the actual state will get observation value more likely.

The standard PF can achieve the system state prediction with uncertainty representation, but the particles diversity will decrease in the sequential importance sampling (SIS) process. That is the particle with high weight was selected more times, which would lead to so many duplicated points in the sampling results. Consequently, the results could not represent the pdf distribution of the state variables; thus, it will bring the divergence of the prediction result. To solve the undesirable prediction accuracy and precision caused by the particles diversity problem, in this work, the regularized particle filter algorithm is adopted to improve the prediction precision of pdf [25].

2.3 Regularized particle filter algorithm

Regularized particle filter (RPF) [26] is proposed to improve the particle degradation by the SIS. The difference between the RPF and SIS PF is the re-sampling process. The SIS re-samples from the discrete approximate distribution, while the RPF re-samples from the successive approximate distribution. The particles are obtained from the re-sampling of successive approximate distribution by the Eq. (11).

$$\begin{aligned} &(\mathbf{X}_k|\mathbf{Y}_{1:k}) \approx \hat{p}(\mathbf{X}_k|\mathbf{Y}_{1:k}) = \sum_{i=1}^{N} \pi_k^i K_h(\mathbf{X}_k - \mathbf{X}_k^i) \\ &K_h(\mathbf{X}) = \frac{1}{h^{n_x}} K\left(\frac{\mathbf{X}}{h}\right) \end{aligned} \quad (11)$$

Here $K_h(\cdot)$ is a new Kernel function rescaled from symmetric Kernel density function $K(.)$, $h > 0$ is the Kernel width, n_x the dimension of the state vector $\mathbf{X}$, $K(.)$ is symmetric probability density function.

$$\begin{aligned} &\int \mathbf{X}K(\mathbf{X})\mathrm{d}\mathbf{X} = 0 \\ &\int \|\mathbf{X}\|^2 K(\mathbf{X})\mathrm{d}\mathbf{X} < \infty \end{aligned} \quad (12)$$

Comparing the re-sampling process of the RPF algorithm with the standard PF algorithm, additional N times sampling from the Kernel density is addicted for the RPF algorithm. Therefore, the computing complexity

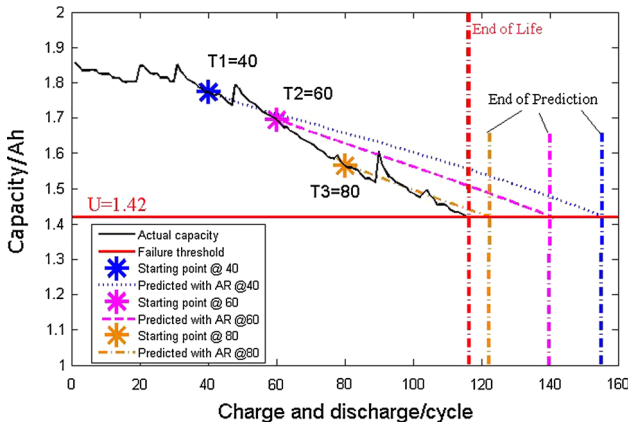

Fig. 1 Battery RUL estimation at different starting points with AR model (NASA Battery No. 05)

remains no remarkable changes of the RPF algorithm. However, when the particles diversity become deficient, the estimation precision of the RPF is superior to the standard PF algorithm. As a result, the RPF can assure the prediction and estimation precision.

3 The proposed fusion framework for lithium-ion battery RUL estimation

3.1 Nonlinear degradation AR algorithm

In this section, the basic AR model is applied to achieve the lithium-ion battery RUL estimation with the long-term time series prediction. Based on the experimental results, the unsuitability for the nonlinear degradation of lithium-ion battery RUL estimation is analyzed. Finally, the nonlinear degradation AR model for battery RUL multi-step prediction is proposed to expect better prognostic performance.

Figure 1 shows the battery RUL estimation result (the Battery No. 05 from NASA PCoE Center [27]) at different starting points with four-order AR model.

In the experiments, the prediction is fulfilled at three different starting points, respectively: $T_1 = 40$ cycles, $T_2 = 60$ cycles and $T_3 = 80$ cycles (marked in Fig. 1). The end-of-life (EoL) of the battery No. 05 is about 116 cycles shown in Fig. 1. We define that when the maximum charging capacity of the battery degrades to the 70 % of its rated capacity, the battery reaches its EoL (In experiment, while the capacity of the battery degrades to 1.42 Ah defined as the EoL). We can find that different prediction results are obtained at different prediction starting points. More quantified result is shown as Table 1. (Here, we conduct the experiments by every 4 cycles.)

Table 1 Comparison of long-term prediction with AR model at different starting points

Starting points	End of prediction (cycle)	RUL prediction result (cycle)	Real RUL value (cycle)	Prediction error (cycle)
20	/	/	108	/
24	158	134	104	30
28	226	198	100	98
32	197	165	96	69
36	162	126	92	34
40	166	126	88	38
44	167	123	84	39
48	170	122	80	42
52	177	125	76	49
56	165	109	72	37
60	150	90	68	22
64	156	92	64	28
68	145	77	60	17
72	136	64	56	8
76	136	60	52	8
80	134	54	48	6
84	129	45	44	1
88	128	40	40	0
92	143	51	36	15
96	134	38	32	6
100	131	31	28	3
104	137	33	24	9
108	130	22	20	2
112	128	16	16	0
116	128	12	12	0
120	133	13	8	5
124	131	7	4	3

From the Table 1, at the early stage ($T = 40$ cycles) and medium-term ($T = 60$ cycles), the RUL prediction results are not satisfied. Although the AR model could be applied to realize trend prediction in time series analysis, the AR model is still a linear modeling method. By analyzing the degradation trend of the lithium-ion battery, we find that with the degradation process evolved, the degradation rate will accelerate with the increasing of cycle number.

So we can conclude that the prediction function with the basic AR model cannot track the "accelerated" degradation process. With the evolvement of the degradation with the charging and discharging, it shows an accelerated degradation trend from the lifetime monitoring data. Especially, while modeling at the early stage and medium stage, the RUL prediction result could not satisfy the actual application.

To solve the poor prediction accuracy and improve the RUL estimation performance with AR model, the

"accelerated" degradation factor should be considered. To implement more precise degradation trend tracking, an accelerated factor could modify the un-matching of the AR model. To check the un-matching phenomenon carefully, we can find that with the degradation process develops (the degradation cycle increases), the degree of the un-matching strengthens.

The accelerated degradation characteristics above can be understood as follows. With the charging and discharging cycle, the inner lithium-ion decreases and the resistance increases. With this degradation process developed, the degradation trend will be accelerated with the increasing of the inner resistance. As a result, the power loss will be gradually increased leading the accelerated degradation process.

With this accelerated degradation factor, the linear AR time series prediction value could be supplemented. Moreover, with this idea, the high efficiency of the AR model could be kept well. According to the analysis above, we propose an improved battery RUL estimation approach with AR model combined with nonlinear degradation process (accelerated degradation process with the cycle increasing). We denote this novel model as nonlinear degradation AR model (ND–AR model). The ND–AR model is defined as follows.

An "accelerated" factor is identified to the AR model output to match the battery degradation process:

$$x_t = K_T \times [\phi_1 x_{t-1} + \phi_2 x_{t-2} + \cdots + \phi_p x_{t-p} + a_t] \tag{13}$$

here the K_T is the "accelerated" factor. Considering the accelerated factor is correlated with the degradation cycle, we define the K_T as follows considering the nonlinear degradation process analyzed above.

$$K_T = \frac{1}{1 + a \times (k + b)} \tag{14}$$

In Eq. (13), k is the prediction step, a and b are the parameters that should be identified with the training data samples, and K_T becomes the time varied accelerated factor with the prediction process.

While the parameters estimation of the AR model is fulfilled, the parameters in Eq. (13) could be obtained by curve fitting or least square estimation.

3.2 Fusion framework with ND–AR model and RPF algorithm

Our motivation is to combine the ND–AR and RPF algorithm together to achieve battery RUL prediction. On the one hand, due to the monitoring data available, while the battery is working, the data-driven method [2, 14] could be used to realize battery cycle life prediction based on the state information. The time series prediction method could be adopted to achieve long-term prediction. On the other hand, due to the inaccessibility of the real measurement value, the long-term predicted value could be utilized as the approximated value of the real value of the lithium-ion battery, so the prediction result by the ND–AR time series model could be as the state observation equation to improve and correct the performance under various operating conditions. Furthermore, the uncertainty representation and states estimation could be obtained by the RPF algorithm. Thus, the fusion framework could realize monitoring and RUL estimation for individual battery by take advantages of both data-driven approach and model-based approach.

The empirical degradation model for the lithium-ion battery described in [3, 4] is applied as the physical model, which is used as the state transition model.

$$C_{k+1} = \eta_C C_k + \beta_1 \exp(-\beta_2 / \Delta t_k) \tag{15}$$

where C_k is the charging capacity in the kth cycle, Δt_k is the rest time interval from the kth cycle to the $(k + 1)$th, and β_1 and β_2 are the parameters to be identified.

Figure 2 shows the schematic diagram of the proposed fusion prognostic framework for the lithium-ion battery RUL estimation.

The fusion prognostic framework of the ND–AR model and RPF algorithm for lithium-ion battery cycle life estimation is as follows.

Definition: Parameters β_1 and β_2 in lithium-ion battery empirical degradation model, prediction starting point T, prediction period k, length of training data set length in ND–AR model, particles number N, process noise covariance R of the $\mathbf{w}_k$ in state transition equation observed noise covariance Q of the $\mathbf{v}_k$ in observation equation, battery actual capacity value *Capacity*, capacity estimation value *Capout*(k), the threshold of end-of-life U, ND–AR model prediction output ARpredict(k);

Input: *Capacity*;

Output: capacity prediction value Capout(k) in kth step with RPF algorithm as well as its pdf distribution corresponded cycle life value *RUL*;

Firstly, the parameters are obtained by the tracking ability of the RPF algorithm. Then, the ND–AR model is built to realize long-term prediction of the battery capacity, its output is "ARpredict(k)." This prediction result is used as the observation value of the state updating equation of the RPF algorithm. The final prediction result is output by the RPF algorithm. The capacity prediction result *Capout*(k) is output in each step and examined whether it reaches the threshold U. If the *Capout*(k) reaches U, the iteration stops and computes the corresponding *RUL* result and its pdf.

The detailed steps of the fusion prognostic framework are as follows.

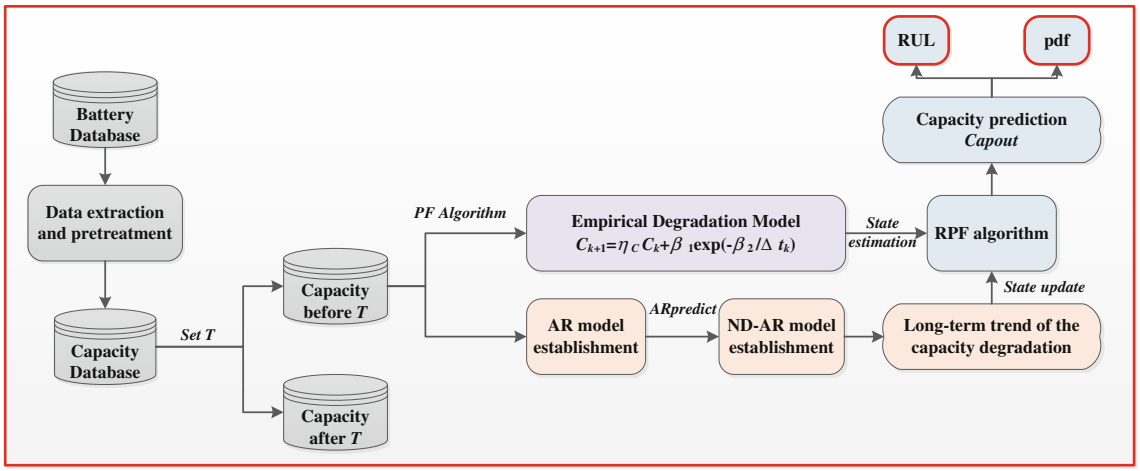

Fig. 2 The schematic diagram of the proposed fusion framework for lithium-ion battery RUL estimation

1. Extract battery capacity data "Capacity" from the battery data set and preprocess the capacity data such as eliminating the outliers and sampling the data with different intervals.
2. Set the starting point of the prediction algorithm T which divides the data into two parts: the historical data whose cycle number is no more than T, we implement the prediction algorithm after cycle T to give the capacity value for each cycle.
3. According to the starting point T, the capacity data before the T cycle are tracked by PF algorithm to determine the unknown parameters β_1 and β_2 in the empirical degradation model.
4. Determine the order of the AR/ND–AR model according to the AIC criterion and model with the historical data, the determined order of AR/ND–AR model and K_T, then complete parameters estimation by Burg algorithm.
5. Estimate the capacity ARpredict(k) for each cycle by using the ND–AR model we built to output the long-term trend of the capacity degradation which will be used as the observed values in the following RPF algorithm.
6. Initialize the RPF algorithm, set some relevant parameters during the battery RUL prediction process:
   - The number of particles N
   - The process noise $\mathbf{w}_k$'s covariance R and the observation noise $\mathbf{v}_k$'s covariance Q in the RPF algorithm
   - The failure threshold to the EoL U
7. Use the RPF algorithm to predict the cycle life of the lithium-ion battery, the brief procedure is as follows:
   - Initialize the particle set, $k = 1$, and generate particles
   - Start the iteration process and obtain system state value $\mathbf{X}_k^i$ according to Eq. (15)
   - Importance sampling: $\widetilde{x}_k^{(i)} = \pi(x_k|x_{0:k-1}^{(i)}, y_{1:k})$ and calculate the observed value $\mathbf{Y}_k^i$ with the ND–AR output
   - Calculate the weight of the particles and normalize the weight $\widetilde{w}_k^{(i)}$
   - Perform the re-sampling process: calculate the empirical covariance matrix S_k and then compute D_k that meets $D_k D_k^T = S_k$; For $i = 1, 2, \ldots N$, sample from a discrete distribution to obtain $j(i)$, the discrete distribution meets $P(j(i) = l) = w_k^{(l)}$, $l = 1, 2, \ldots N$; for $i = 1, 2, \ldots N$, $\breve{x}_{0:k}^{(i)} = \widetilde{x}_{0:k}^{j(i)}$ and $\breve{w}_k^{(i)} = N^{-1}$; for $i = 1, 2, \ldots N$, Epanechnikov Kernel function $\varepsilon^i \sim K$ and let $\breve{x}_{0:k}^{(i)*} = \breve{x}_{0:k}^{j(i)} + h_{opt} D_k \varepsilon^i$
   - Generate the state estimation of the battery capacity $Capout_k = \sum_{i=1}^{N} \widetilde{x}_{0:k}^{(i)} \widetilde{w}_k^{(i)}$
   - Let $k = k + 1$, repeat the procedure above orderly and update the capacity of the battery interactively according to the state space model to output a estimated state $Capout(k)$ for each cycle.
8. Judge whether the value of $Capout(k)$ reaches the threshold U as the EoL, if it is, then calculate the RUL prediction result of the cycle life: $RUL = k$.
9. According to the corresponding relation among the pdf of the battery capacity value and the cycle life, calculate the pdf of RUL and output the final result.

The detailed flowchart of the proposed fusion framework for lithium-ion battery RUL estimation is shown as Fig. 3.

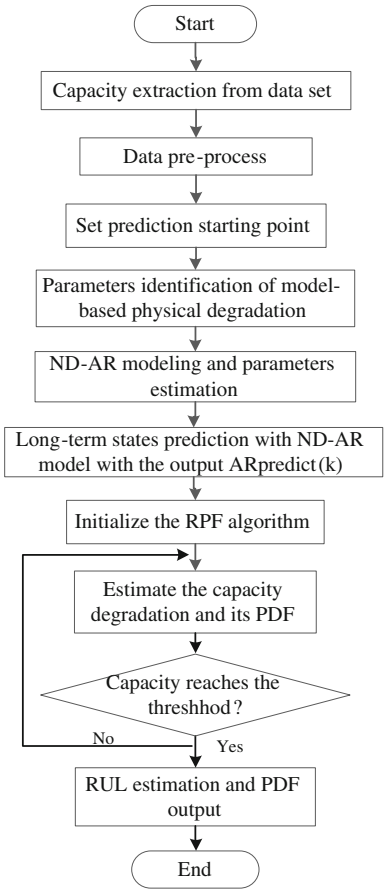

Fig. 3 Fusion prognostic framework for lithium battery cycle life estimation based on ND–AR model and RPF Algorithm

Note that with the update of the online data sample, the ND–AR model could be dynamically adjusted if it is needed. As a result, the observed value for the RPF algorithm could be updated to increase the prediction precision.

4 Experiments analysis and evaluation

4.1 Battery data set

To evaluate the proposed methods, we adopt two types of battery data sets. With different battery data sets under various experimental conditions, the adaptability and effectiveness of the proposed method can be verified and proved adequately.

4.1.1 NASA PCoE battery data set [10, 27]

The first lithium-ion battery data set we utilize is from NASA Prognostics Center of Excellence (PCoE). The battery data set is tested and obtained in the NASA PCoE.

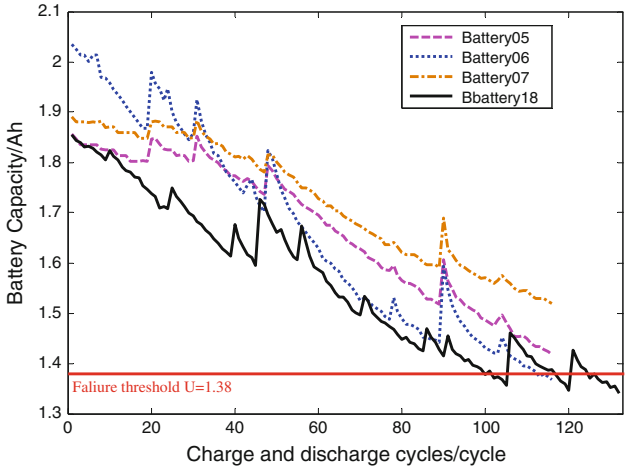

Fig. 4 Capacity degradation curves of lithium-ion battery in NASA PCoE (Battery No. 05, 06, 07 and 18 are involved)

The lithium-ion batteries were tested under certain condition (with the temperature +25 °C) to measure the degradation of the capacity.

- The 2 Ah batteries are charging with the charging current 1.5 A until the batteries voltage reaches 4.2 V.
- The batteries are discharging with the discharging current 2 A until the batteries voltage reaches 2.5 V.
- The batteries impedances are tested by EIS with the scanning frequency from 0.1 Hz to 5 kHz.

We select the capacity as the health indicator (HI) of the performance degradation for the lithium-ion battery. When the lithium-ion battery reaches its EoL, that is the battery charging capacity degraded to about 70 % of rated capacity. In the experiments, the nominal capacity of lithium-ion battery is 2 Ah and the failure threshold is set to 1.38 Ah. If the battery capacity reaches 1.38 Ah, the RUL estimation experiment ends. The lithium-ion battery capacity degradation is shown as Fig. 4.

4.1.2 CALCE lithium-ion battery data set of University of Maryland

The second lithium-ion battery data set is from CALCE (The Center for Advanced Life Cycle Engineering, The University of Maryland). The lithium-ion batteries are tested to discover the degradation of the capacity. The cycling of the batteries is implemented with the Arbin BT2000 battery testing system under room temperature. The 1.1 Ah rated capacity of batteries is used in the experiment with the discharging current (0.55 A, the discharging speeds is 0.5C) [2]. The battery capacity degradation of various batteries is shown as Fig. 5.

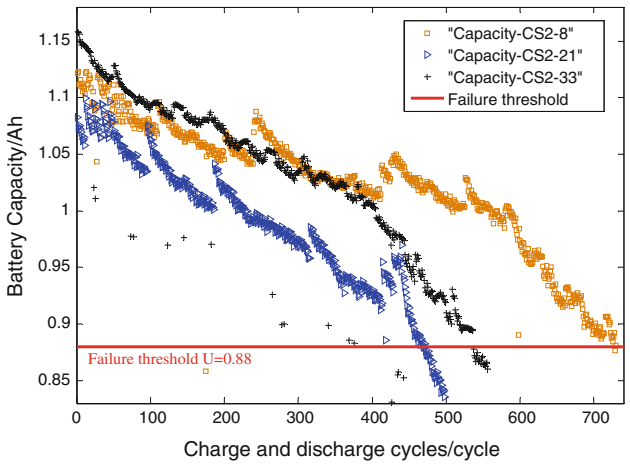

Fig. 5 Capacity degradation curves of lithium-ion battery in CALCE (Battery No. CS2-8, No. CS2-33, No. CS2-21 are involved)

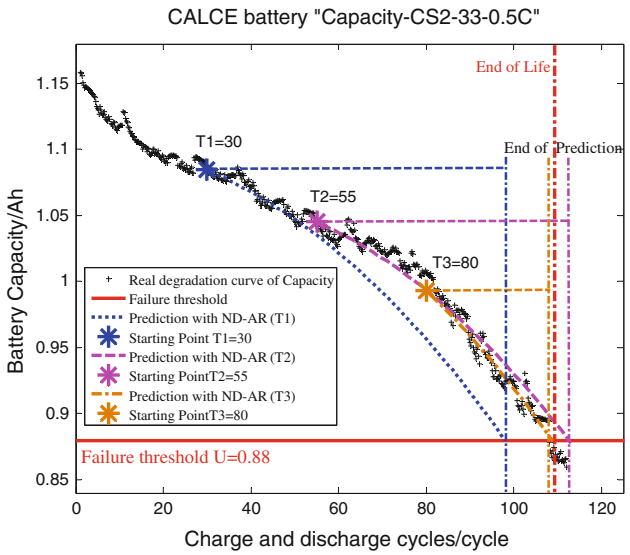

Fig. 6 RUL estimation at different starting points with the ND–AR model (CALCE battery Capacity-CS2-33-0.5C)

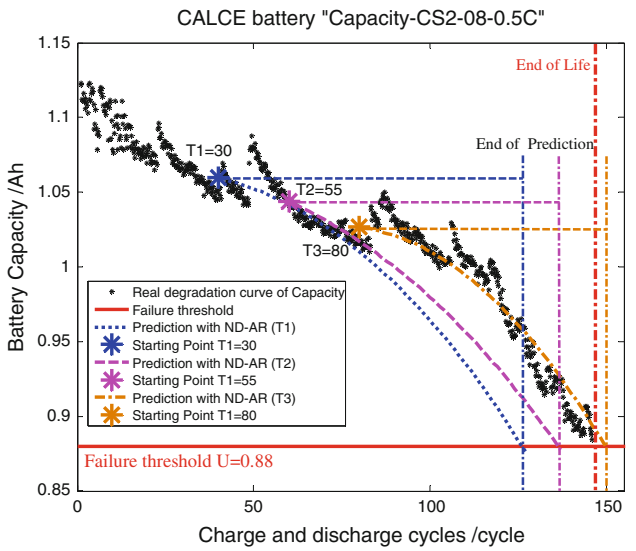

Fig. 7 RUL estimation at different starting points with the ND–AR model (CALCE battery Capacity-CS2-08-0.5C)

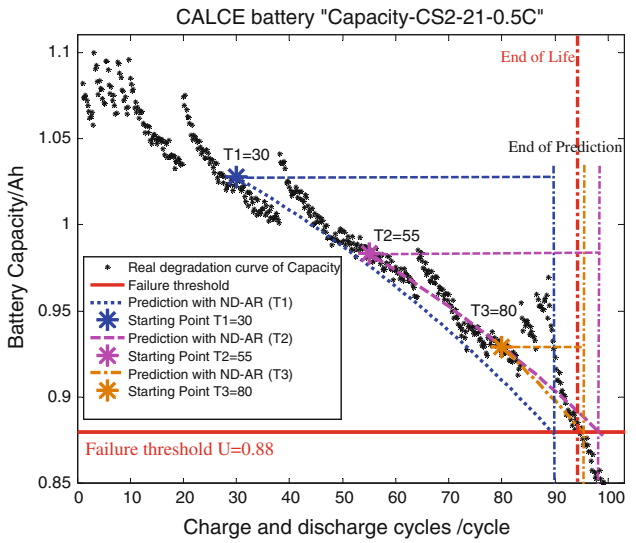

Fig. 8 RUL estimation at different starting point with the ND–AR model (CALCE battery Capacity-CS2-21-0.5C)

4.2 Battery RUL estimation with ND–AR model

We first evaluate the effectiveness of the proposed ND–AR model for capacity degradation time series of lithium-ion batteries. Then, the fusion prognostic model with ND–AR and RPF algorithm would be verified. To briefly introduce the evaluation of the ND–AR model, here we only introduce the prediction results with the CALCE battery data. (And the predicted results are indicated through comparison with NASA PF algorithm in Sect. 4.4.)

The parameters of AR model containing the order p and other parameters are determined using the same method as described in Sect. 3.1. The order p value equals to 4 while the model gets best prediction performance. With the curve fitting method, the parameters a and b in the ND–AR model are estimated, $a = 1.5\text{e}{-7}$, $b = 100$. The other parameters are obtained with Burg algorithm to the observed capacity degradation BCm (1: T) with the modeling process.

Figures 6, 7 and 8 show the prediction result for various lithium batteries capacity degradation data with the ND–AR model proposed in this paper. From the prediction results for the three batteries, we can conclude that the capacity degradation process under different testing and operating condition is forecasted precisely with the ND–AR model. The prediction and estimation of RUL will be beneficial for the system management and maintenance of the lithium-ion batteries.

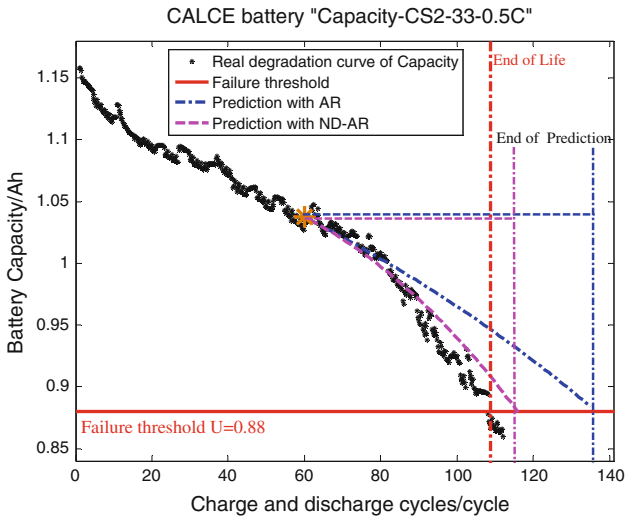

Fig. 9 Comparison of RUL estimation with the ND–AR model and basic AR model (CALCE battery Capacity-CS2-21-0.5C)

We compare the battery RUL estimation results with the ND–AR model and the basic AR model to indicate the efficiency of the novel ND–AR model. Figure 9 gives the comparison of the RUL prediction with the proposed ND–AR model and basic AR model.

From Fig. 9, we can conclude that compared to the basic AR model, the proposed ND–AR model can realize more satisfied prediction result at the same starting point.

To evaluate and compare experimental results quantitatively, we adopt the mean absolute error (MAE) and root mean square error (RMSE) and error of RUL estimation to analyze the prediction results with two methods. The definitions of evaluated parameters are as follows.

The MAE:

$$\mathrm{MAE} = \frac{1}{n}\sum_{i=1}^{n} |x(i) - \bar{x}(i)| \tag{14}$$

The RMSE:

$$\mathrm{RMSE} = \sqrt{\frac{1}{n}\sum_{i=1}^{n} [x(i) - \bar{x}(i)]^2} \tag{15}$$

The error of RUL:

$$E_{\mathrm{RUL}} = \left| RUL_{\mathrm{real}} - RUL_{\mathrm{prediction}} \right| \tag{16}$$

Here, n the number of prediction data set, $x(i)$ is the real value of testing and monitoring of battery capacity, $\bar{x}(i)$ is the prediction value. In the experiments, k is the prediction steps from the starting point T.

The detailed results and quantitative comparison are shown as Table 2, in which the average statistical results with different starting points are involved.

From Table 2, we can find that the predictions MAE, RMSE and error of RUL of the ND–AR model are superior to the AR model for various lithium-ion batteries. Furthermore, the long-term prediction performance is satisfied at different starting point which shows the effectiveness and efficiency of the optimized ND–AR model. (The three batteries RUL estimation error are all within 10 cycles.)

Table 2 Comparison of AR model and ND–AR model for battery RUL estimation

Index of batteries	CALCE No. CS2-8	CALCE No. CS2-21	CALCE No. CS2-33
MAE of ND–AR	0.0060	0.0057	0.0066
MAE of AR	0.0304	0.0287	0.0317
RMSE of ND–AR	0.0113	0.0105	0.0126
RMSE of AR	0.0349	0.0316	0.0397
E_{RUL} of ND–AR	10	8	7
E_{RUL} of AR	34	27	28

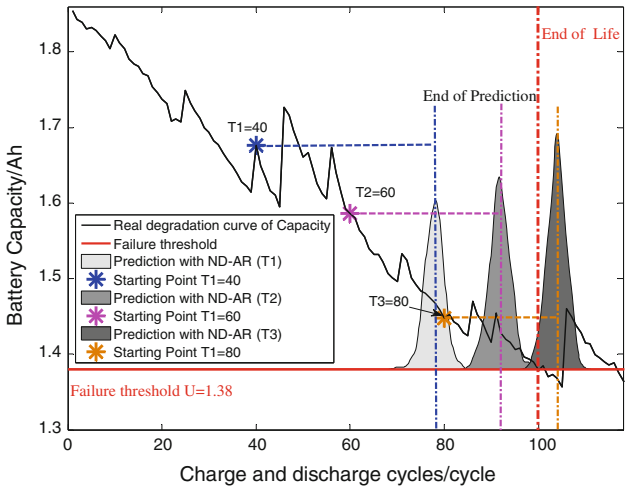

Fig. 10 Battery RUL estimation results based on fusion prognostics with PDF uncertainty representation (at starting points $T_1 = 40$, $T_2 = 60$, $T_3 = 80$)

4.3 Battery RUL prediction with fusion prognostics

With the data-driven optimized ND–AR model, we can realize more satisfied RUL prediction performance. However, only with the single point prediction result, the maintenance reference for the industrial application is limited due to lack of uncertainty representation ability. We evaluate and verify the fusion prognostic framework for the lithium-ion battery RUL estimation.

Here, we first use the NASA PCoE battery data set to implement the experiments. The related parameters are set as: the prediction starting points $T = 60$ cycles, the end-of-life (EoL) for batteries $U = 1.38$ Ah, the number of

Table 3 Comparison of the RUL prognostic results at different starting points

Starting points	End of prediction/cycle	RUL prediction/cycle	Prediction error/cycle
20	63	43	37
30	73	43	27
40	77	37	23
44	81	37	19
48	81	33	19
52	86	34	14
56	84	28	16
60	88	28	12
64	89	25	11
68	93	25	7
72	92	20	8
76	97	21	3
80	98	18	2
90	98	8	2

particles $N = 500$, state initial value of the battery capacity $C_0 = \text{Capacity}(T) = 1.586$ Ah $(T = 60$ cycles), the covariance of process noise $\mathbf{w}_k$ $R = 0.0001$, the covariance of the measure noise $\mathbf{v}_k$ $Q = 0.0001$. The combined ND–AR model and RPF algorithm RUL prediction results are shown as Fig. 10.

In Fig. 10, the center point of the pdf represents the accuracy of prediction, while the width of the pdf represents the precision of prediction. With the prediction starting point moves forward, the center point of the pdf in prediction results gets closer to the actual end-of-life (100 cycles). At the same time, the width of the pdf distribution becomes more centralized and the scatter of pdf becomes smaller, which means the uncertainty of the prediction results decreased and the RUL estimation performance improved.

As shown in Fig. 10, the actual EoL of the battery No. 18 is 100 cycles. While the prediction starting point $T = 60$ cycles, the actual RUL is: $RUL\_true = 100cycle - T = 40cycle$. The predicted life is 83 cycles. So the estimated RUL value is: $RUL\_prediction = 83cycle - T = 23cycle$, prediction error is $RUL\_error = |23cycle - 40cycle| = 17cycle$.

The quantitative RUL prediction results (at early cycle life, medium cycle life and latter cycle life as the prediction starting points) are shown as Table 3. (Here, we conduct the experiment by every 4 cycles during the medium degraded process, such as at cycles 44, 48, 52, etc. Moreover, we implement experiment by every 10 cycles at the early stage, such as 20, 30, because the degraded prediction is difficult and of less scientific reference for users. The same setting is adopted during the latter degraded period due to that the predicted value is very close to the actual value of RUL.)

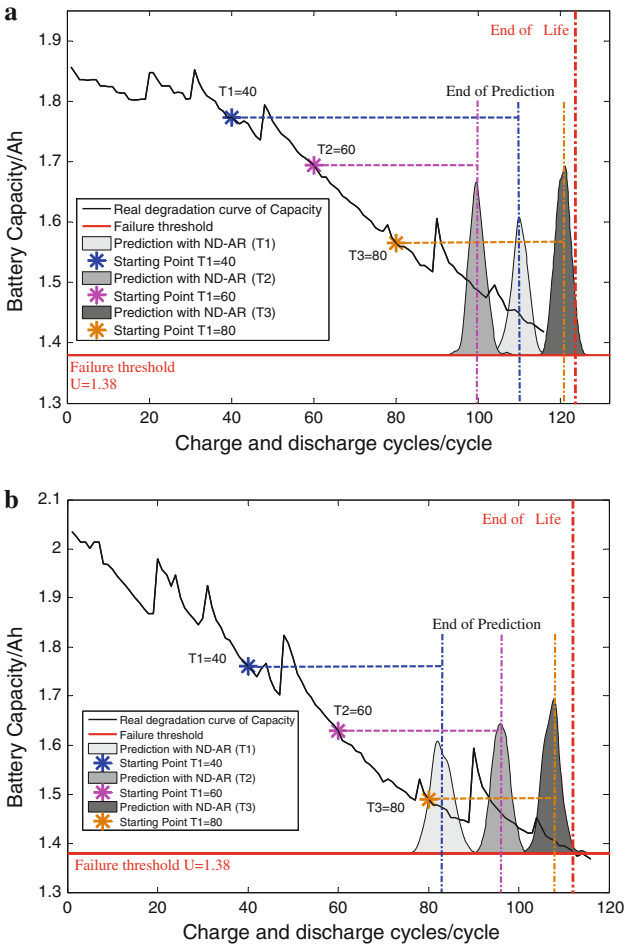

Fig. 11 Prediction results with PDF for Battery No. 05 and No. 06: **a** Battery No. 05 RUL prediction; **b** Battery No. 06 RUL prediction

From Table 3, when the starting points are 40 cycles, 60 cycles and 80 cycles, respectively, the end of prediction (EoP) is 77 cycles, 88 cycles and 98 cycles, gradually be closer to the actual cycle life (100 cycles). By analyzing the experimental results, the prediction accuracy and precision at the early stage is much lower. However, for actual industrial application, the operator is not so attention to the early stage prediction results.

By examining Table 3 and Fig. 10, the predicted remaining cycle life of lithium-ion batteries could be obtained precisely at the medium and latter stages. Moreover, the integration of uncertainty with the prediction RUL results is represented by its pdf. The precise and accurate prediction RUL result and its pdf uncertainty representation could be scientific reference for the operators and decision makers. For different industrial requirements, the relative boundary of probability could be set to take different levels of attentions for different system

Table 4 RUL prediction results for other batteries with the fusion approach

Battery index	Starting points/cycle	EoP/cycle	RUL/cycle	Error/cycle
Battery No. 05 (=128)	20	70	50	58
	30	91	61	37
	$T_1 = 40$	100	60	28
	44	102	58	26
	48	108	60	20
	52	105	53	23
	56	108	52	20
	$T_2 = 60$	110	50	18
	64	112	48	16
	68	118	50	10
	72	116	44	12
	76	122	52	4
	$T_3 = 80$	120	40	8
	90	127	37	1
	100	132	32	4
Battery No. 06 (=112)	20	69	49	43
	30	76	46	36
	$T_1 = 40$	84	44	28
	44	86	42	26
	48	88	40	24
	52	94	42	18
	56	93	37	19
	$T_2 = 60$	96	36	16
	64	97	33	15
	68	103	25	9
	72	106	24	8
	76	105	29	7
	$T_3 = 80$	108	28	4
	90	113	23	1
	100	112	12	0

maintenance. With predicted probability increased, the appropriate maintenance strategy could be adopted combined with the expert knowledge.

To verify the efficiency of the proposed approaches, we also implemented prediction experiment for other lithium-ion batteries. The lithium-ion Battery No. 05 and Battery No. 06 of NASA PCoE are used to evaluate the RUL prognostic method. (In the same battery group, the capacity of the Battery No. 07 has not reached its threshold involving in the battery state monitoring data set. Thus, in the experiment, we did not use this lithium-ion battery data set.) The detailed experimental results are shown as Fig. 11.

The quantitative battery cycle life prediction results are as shown as Table 4. (The same experimental setting is adopted as the Table 3.)

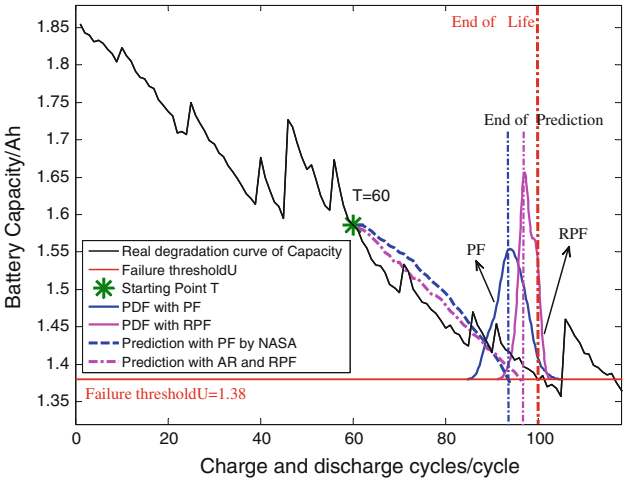

Fig. 12 RUL estimation results with proposed fusion prognostic algorithm and standard PF algorithm

With the experimental results and analysis above, the RUL estimation accuracy and precision is more satisfied at the medium and latter cycle life for the Battery No. 06 and Battery No. 07. Furthermore, the uncertainty with the prediction results shows prospective for the industrial application especially for the battery management and maintenance.

The fusion prognostic method with the NASA battery data set and CALCE battery data set (the detail experimental result with the CALCE battery data set as well as the comparison with other similar methods will be introduced in Sect. 4.4) indicates that the combined approach of ND–AR model and RPF algorithm can realize high precision RUL prediction as well as its uncertainty representation and management. Moreover, the precision of uncertainty representation is also improved with the proposed fusion approach and optimized PF algorithm.

4.4 Comparison with other prognostics approaches

To further verify the efficiency of the proposed methods, we also realize the comparison with other two types of work: One is the battery RUL prediction based on PF algorithm by NASA [28] and the other is the prediction with D-S evidence theory and Bayesian Monte Carlo method proposed by Wei He et al. [2] of CALCE.

4.4.1 RUL prognostics comparison I

We first compared the RUL estimation performance with the proposed fusion approach and PF algorithm. In the experiment, the NASA Battery No. 18 was adopted to achieve comparison and evaluation. The parameters are set the same with the experiment in Sect. 4.3 (Fig. 12).

In order to completely compare the different prognostics methods and give the quantitative performance, in this

Table 5 Prediction comparison with PF and fusion prognostic approach

Approaches	MAE/Ah	RMSE/Ah	RUL error/cycle	$\hat{N}_{\text{eff}}$
NASA_PF	0.0522	0.0378	11	382
ND-AR_RPF	0.0335	0.0246	9	413

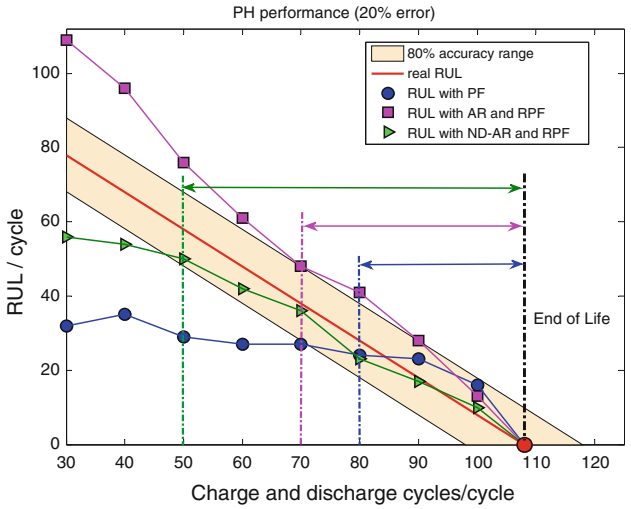

Fig. 13 Battery RUL prediction results and its PH performance

work, we used four types of criteria to evaluate the predicted algorithm in this experiment: MAE, RMSE, RUL prediction error (defined as Eqs. 14–16) and valid samples $\hat{N}_{\text{eff}}$ in PF algorithm. The valid samples in PF algorithm $\hat{N}_{\text{eff}}$ is defined as:

$$\hat{N}_{eff} = \frac{1}{\sum_{i=1}^{N} (\tilde{w}_k^{(i)})^2} \tag{17}$$

From Fig. 12 and Table 5, with the combined ND–AR and RPF algorithm, the battery RUL prediction MAE and RMSE is much smaller than the standard PF algorithm. This represents the dispersion degree of particles is lower. The pdf distribution shows the high peak and narrow range, which means that the valid samples of the RPF algorithm is also superior to the PF algorithm. Thus, the uncertainty of the prediction is superior to the NASA PF RUL framework.

More evaluation experiments are achieved to further analyze the proposed approaches and other battery RUL prediction methods. Here, we compared the followed three types of RUL estimation methods: standard PF by NASA, fusion AR and RPF approach (as AR_RPF), and fusion improved ND–AR and RPF approach (as ND-AR_RPF).

The "Capacity-CS2-33" battery data set of CALCE is used in the experiment. The parameters for experiments are as follows: prediction starting points $T_i = \{30, 40, \ldots 90, 100\}$, the number of particles

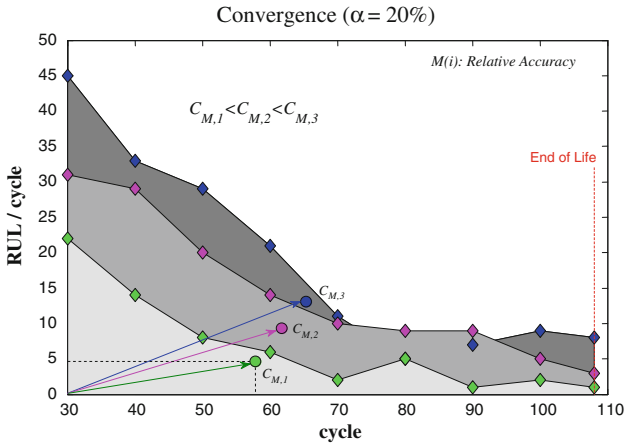

Fig. 14 Convergence performance with various approaches for battery RUL estimation

$N = 500$, the noise covariance $R = 0.0004$ and $Q = 0.0004$, the EoL (capacity) $U = 0.88$ Ah. We applied five evaluation criteria: Prognostic Horizon (PH), $\alpha-\lambda$ Accuracy, Relative Accuracy (RA), Cumulative Relative Accuracy (CRA) and Convergence to compare the efficiency and performance of the RUL prediction methods [29]. The detailed results are shown as Fig. 13.

From Fig. 13, we can conclude that the RUL prediction with our proposed methods is better than the standard PF algorithm. Especially, at the early prediction stage, the prediction error is small with the PH performance. At the same time, for later prediction stage, the prediction value is almost following at the error limits and very closer to the actual cycle life. The similar conclusion could be obtained as the Fig. 14 (Convergence).

In Fig. 14, the Euclidean distance $C_{M,1}, C_{M,2}, C_{M,3}$ is as the Convergence performance for three methods (corresponded to Standard PF, AR_RPF and ND-AR_RPF, respectively). The specific regional center coordinates are as follows: $x_{C,1}, y_{C,1} = 65.33, 13.09$, $x_{C,2}, y_{C,2} = 61.77, 9.36$, $x_{C,3}, y_{C,3} = 57.87, 4.68$.

The result above indicates that the performance of proposed optimized ND–AR model and RPF algorithm is the best in convergence among the three approaches. The other quantitative criteria are shown as Fig. 15 and Table 6.

From Fig. 15 and Table 6, we can find that the PH performance: $PH_{ND-AR\_RPF} < PH_{AR\_RPF} < PH_{PF}$. The combined ND–AR model and RPF algorithm first dropped to the given intervals ($a = 20$ %). The same conditions could be obtained for the criteria of RA, CRA and CM. All the prediction performance criteria above verified that the proposed method could realize satisfied prediction precision and accuracy compared to the standard PF and fusion AR and RPF method.

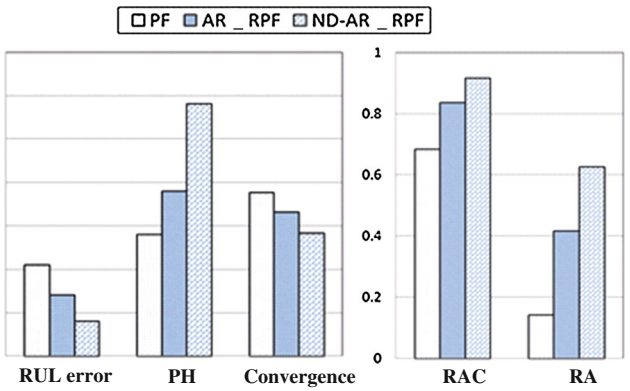

Fig. 15 Quantitative evaluation and comparison of different approaches

Table 6 Quantitative comparison and evaluation of different approaches

Approaches	RUL error $T = 60$ cycle	PH (cycle)	RA ($\lambda = 0.5$)	CRA ($\lambda = 0.5$)	C_M
PF	21	28	0.6842	0.1429	37.6820
AR_RPF	14	38	0.8361	0.4175	33.1298
ND-AR_RPF	8	58	0.9174	0.6263	28.2591

4.4.2 RUL prognostics comparison II

Wei He et al. [2] applied Dempster-Shafer evidence theory (DST) and Bayesian Monte Carlo method (denoted as D_B method in the experiment) to achieve lithium-ion battery RUL prediction. We compared the proposed novel approach (denoted as ND-AR_RPF) with the prediction method by Wei He. We implemented battery RUL estimation to the CALCE data, in which the Battery No. B4 is used to evaluate these two RUL methods. In the experiment, the data set was sampled by every five data points to simple the capacity data. The other related parameters as set as: the prediction starting point $T = 50(\times 5)$ cycle, the capacity threshold of the EoL $U = 0.88$ Ah, the number of the particles $N = 500$, the covariance of process noise W_k $R = 0.0001$, the covariance of the measure noise V_k $Q = 0.0001$, state initial value of the battery capacity $C_0 =$ Capacity $(T) = 1.056$ Ah ($T = 50 \times 5$ cycle). The experimental results are shown as Fig. 16.

We can see from Fig. 16 that the actual EoL is $112(\times 5)$ cycle for the CALCE Battery No. B4, while the prediction result by the proposed method is $111(\times 5)$ cycle, and the uncertainty representation with the RPF algorithm is $106–120(\times 5)$ cycle, the quantitative comparison results is shown as Table 7. (The prediction result of D_B method could be referred in [2].)

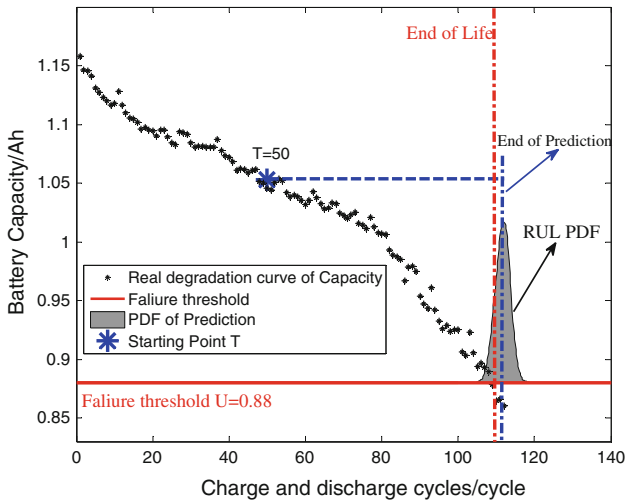

Fig. 16 Battery RUL estimation with ND-AR_RPF algorithm (CALCE Battery No. B4)

Table 7 RUL estimation results with proposed ND-AR_RPF algorithm and D_B method

Methods	RUL error/cycle	PDF intervals/cycle	PDF ranges/cycle
ND-AR_RPF	5	530–600	70
D_B	7	550–670	120

It can be concluded from the Table 7 that the RUL prediction error is smaller, which indicated that the proposed method is superior to the prediction method by Wei He et al. Considering the uncertainty quantitative result, with the RPF algorithm, we obtain the uncertainty distribution interval equals to 70 cycles, which is much smaller than the 120 cycles with the D_B methods. It shows that the point estimation performance and the uncertainty quantitative representation performance, the proposed methods are much better.

5 Conclusion and future work

This paper explores an improved nonlinear degradation autoregressive (ND–AR) model for lithium-ion battery RUL estimation. A battery RUL prognostic framework of fusion ND–AR model and RPF algorithm is proposed to realize various lithium-ion batteries RUL estimation. The main contribution of this research can be concluded that: (1) based on low computing complexity AR time series model, the "accelerated" nonlinear degradation feature of the battery capacity fade is analyzed based on experiments. (2) A nonlinear degradation factor is extracted to combine with standard AR time series model to realize better RUL

estimation result and more precisely prediction performance could be fulfilled. (3) With RPF prediction algorithm, a data-driven ND–AR method is applied as the observation equation. As a result, the state tracking and predicting ability is improved. (4) Fusion prognostic framework with ND–AR model and RPF algorithm is implemented to realize various lithium-ion batteries RUL estimation. (5) The combined approach achieves batteries RUL uncertainty representation and management.

With the experiment, we can conclude that the improved model is suitable for cycle life estimation of the lithium battery. This proposed fusion lithium-ion battery RUL prognostic framework shows better prospective in industrial application comparing with RUL prediction based on other RUL prediction methods. Moreover, the modeling of the fusion method is relative simple. The framework can be used as a practical technique solution for the lithium-ion battery RUL estimation. The proposed method is not only suitable for battery cycle life prediction with small sample size, but also of the ability uncertainty representation and management. Compared to the standard PF algorithm and other statistical methods, more accurate uncertainty representation could be provided, which proved great scientific reference for the maintenance and management of complex systems.

In the future, we will consider the uncertainty representation ability of the proposed ND–AR model (data-driven prognostics). The dynamic parameters training and models fusion for battery with complex operating condition should be focused in our future work. Furthermore, the capacity regeneration modeling and low depth of discharging (DOD) modeling for precise RUL prediction are focusing to improve applicable capability.

Acknowledgments This research work is supported partly by National Natural Science Foundation of China (61301205), Natural Scientific Research Innovation Foundation in Harbin Institute of Technology (HIT.NSRIF.2014017), Research Fund for the Doctoral Program of Higher Education of China (20112302120027), the twelfth government advanced research fund (51317040302). The author would also express his sincere thanks to Dr. Wei He at CALCE of The University of Maryland and Dr. Eden Ma at PHM Center of City University of Hong Kong for their help on the CALCE battery data set. The authors would also like to thank anonymous reviewers for their valuable comments.

References

1. Zhang J, Lee J (2011) A review on prognostics and health monitoring of Li-ion battery. J Power Sources 196(15): 6007–6014
2. He W, Williard N, Osterman M, Pecht M (2011) Prognostics of lithium-ion batteries based on Dempster-Shafer theory and the Bayesian Monte Carlo method. J Power Sources 196:10314–10321
3. Goebel K, Saha B, Saxena A, Celaya JR, Christophersen JP (2008) Prognostics in battery health management. IEEE Instrum Meas Mag 8:33–40
4. Saha B, Goebel K, Poll S, Christophersen J (2009) Prognostics methods for battery health monitoring using a Bayesian framework. IEEE Trans Instrum Meas 58(2):291–297
5. Liu J, Wang W, Golnaraghi F (2009) A multi-step predictor with a variable input pattern for system state forecasting. Mech Syst Signal Process 23:1586–1599
6. Peng Y, Liu D, Peng X (2010) A review: prognostics and health management. J Electron Meas Instrum 24(1):1–8
7. Si XS, Wang W, Hu CH, Zhou DH (2011) Remaining useful life estimation: a review on the statistical data driven approaches. Eur J Oper Res 213(1):1–14
8. Luo J, Andrew B, Krishna P, Liu Q, Shunsuke C (2003) An interacting multiple model approach to model-based prognostics. In: Proceedings of IEEE international conference on system man and cybernetics. Washington, DC, pp 189–194
9. Pecht M, Jaai R (2010) A prognostics and health management roadmap for information and electronics-rich systems. Microelectron Reliab 50:317–323
10. Saha B, Goebel K, Christophersen J (2009) Comparison of prognostic algorithms for estimating remaining useful life of batteries. Trans Inst Meas Control 31:293–308
11. Olivares BE, Cerda Munoz MA, Orchard ME, Silva JF (2013) Particle-filtering-based prognosis framework for energy storage devices with a statistical characterization of state-of-health regeneration phenomena. IEEE Trans Instrum Meas 62:364–376
12. Orchard ME, Hevia-Koch P, Zhang B, Tang L (2013) Risk measures for particle-filtering-based state-of-charge prognosis in lithium-ion batteries. IEEE Trans Ind Electron 60:5260–5269
13. Liu D, Pang J, Zhou J, Peng Y (2013) Prognostics for state of health estimation of lithium-ion batteries based on combination Gaussian process functional regression. Microelectron Reliab 53:832–839
14. Liu J, Saxena A, Goebel K, Saha B, Wang W (2010) An adaptive recurrent neral network for remaining useful life prediction of lithium-ion batteries. In: Proceedings of annual conference of the prognostics and Health Management Society, Portland, Oregon, USA
15. Liang Y, Liang X (2006) Improving signal prediction performance of neural networks through multi-resolution learning approach. IEEE Trans Syst Man Cybern B 36:341–352
16. Alvin JS, Craig F, Pritpal S, Terrill A, David ER (1999) Determination of state-of-charge and state-of-health of batteries by fuzzy logic methodology. J Power Sources 80(1–2): 293–300
17. Kozlowski JD (2003) Electrochemical cell prognostics using online impedance measurements and model-based data fusion techniques. In: IEEE aerospace conference, Big Sky, Montana
18. Liu J, Wang W, Ma F, Yang Y, Yang C (2012) A data-model-fusion prognostic framework for dynamic system state forecasting. Eng Appl Artif Intel 25:814–823
19. Saha B, Poll S, Goebel K (2007) An integrated approach to battery health monitoring using bayesian regression and state estimation. In: IEEE Autotestcon, Baltimore, MD, USA
20. Xing Y, Ma EWM, Tsui KL, Pecht M (2013) An ensemble model for predicting the remaining useful performance of lithium-ion batteries. Microelectron Reliab 53:811–820
21. Fan J, Yao Q (2003) Nonlinear time series: nonparametric and parametric methods. Springer, New York
22. Akaike H (1974) A new look at the statistical model identification. IEEE Trans Automat Contr 19:716–723
23. Simon D (2006) Optimal state estimation: Kalman, H Infinity and Nonlinear Approaches. Wiley, New Jersey

24. Gordon NJ, Salmond DJ, Smith AFM (1993) Novel approach to nonlinear/non-Gaussian Bayesian state estimation. In: IEEE proceedings on radar and signal processing, pp 107–113
25. LeGland F, Musso C, Oudjane N (1998) An analysis of regularized interacting particle methods for nonlinear filtering. In: Proceedings of the IEEE European workshop on computer intensive methods in control and data processing. Prague, Czech Republic, pp 167–174
26. Arulampalam MS, Maskell S, Gordon N, Clapp T (2001) A tutorial on particle filters for online nonlinear/non-Gaussian Bayesian tracking. IEEE Trans Signal Process 50:174–188
27. Saha B, Goebel K (2007) Battery data set, NASA Ames prognostics data repository, [http://ti.arc.nasa.gov/project/prognostic-data-repository], NASA Ames, Moffett Field, CA, USA
28. Saha B, Goebel K (2009) Modeling li-ion battery capacity depletion in a particle filtering framework. In: Annual conference of the prognostics and health management society, San Diego, CA, USA
29. Saxena A, Celaya J, Saha B, Saha S, Goebel K (2009) Evaluating algorithmic performance metrics tailored for prognostics. In: Proceedings of IEEE aerospace conference, Big Sky, MO, USA